DECAY STUDIES OF NEW NEUTRON DEFICIENT ISOTOPES IN THE RANGE OF ELEMENTS BETWEEN GADOLINIUM AND LEAD

S. Hofmann, G. Münzenberg, W. Faust, F. Heßberger, W. Reisdorf, J.R.H. Schneider, and P. Armbruster

Gesellschaft für Schwerionenforschung mbH., Darmstadt

K. Güttner and B. Thuma

II. Physikalisches Institut, Universität Gießen, Gießen

Abstract

Very neutron deficient isotopes below lead were produced with beams of ^{58}Ni, ^{92}Mo, and ^{107}Ag accelerated by the linear accelerator UNILAC. After separation from the projectile beam by the velocity filter SHIP, the fusion products were implanted with their full recoil energy into an array of position-sensitive detectors. This array is part of a detector system developed for investigation of decay modes of rare isotopes. In a compact geometry α,p,β,γ decay and fission can be observed. With a newly developed position and time correlation technique parent daughter relationships, half lives, and α branching ratios of a large number of isotopes could be determined. Two new α emitting isomeric states could be identified in ^{155}Lu and ^{156}Hf. The energies of the excited states are (1798 $\pm$ 12) keV in ^{155}Lu and (1977 $\pm$ 18) keV in ^{156}Hf, the half-lives are (2.6o $\pm$ o.o7)ms and (444 $\pm$ 17)μs, respectively. Compared to the ground state transitions, a hindrance of $1o^5$ can be deduced for both transitions, possibly indicating orbital angular momenta of the order of 1o $\hbar$ for the α emitting states. The isomers are proposed to belong to shell model isomers beyond ^{146}Gd. A low energetic line at 1.19 MeV was found in the particle spectra taken in reactions of ^{58}Ni +^{96}Ru $\rightarrow ^{154}$Hf. It is tentatively assigned to a proton decay of the new isotope ^{151}Lu.

1. Introduction

The systematics of decay properties of neutron deficient isotopes in the range of elements below lead was increasingly extended in the past years. A review of recent experiments is given in the articles of Hansen[1]) and LeBeyec[2]).

The work presented here has been started at GSI with the aim to obtain comprehensive alpha spectroscopic data for neutron deficient isotopes between the N = 82 and N = 126 neutron shells. Among the methods used to produce very neutron deficient nuclei, two have been particularly successful in the past. Spallation reactions induced by 6oo MeV proton beams have been used at the Isolde Facility[3]). The lack of selectivity of this reaction mechanism which allows to produce copious amounts of many different nuclear species is overcome by the use of on-line electromagnetic isotope separators.

The second method has been using heavy ion (HI) induced fusion reactions together with gas jet techniques. Helium jets have the advantage of combining high efficiency with reasonably fast separation times. For moderately proton rich nuclei the new isotopes are generally identified as (HI, xn) evaporation residues and the reaction mechanism is fairly selective. This identification technique becomes increasingly more ambiguous, however, as the proton drip line is approached. Very neutron deficient excited compound nuclei produced in fusion reactions deexcite by a multitude of evaporation paths due to the increased significance of charged particle emission. Even at relatively moderate excitation energies of (3o-4o)MeV, typical for 3 n reactions, one observes with comparable or higher cross sections 2 np, n2p, 3 p, αnp, n2α etc. products. The excitation functions of all these evaporation products due to the emission of 3 particles are very similar.

A further difficulty which becomes apparent close to the proton drip line and which limits both gas jet and isotope separator techniques is the rapid drop in half lives below the 1oo ms level.

In this work we have used very neutron deficient ions as ^{58}Ni or ^{92}Mo available at the UNILAC accelerator together with an electromagnetic velocity filter[4]) to overcome some of the above difficulties.

The velocity filter efficiently separates projectiles from fusion products in times sufficiently short, typically 1 μs, to allow the investigation of very short lived species. The choice of ions together with neutron deficient targets allows to make weakly excited compound nuclei by fusion that are very close to the region of interest near the proton drip line. It will be shown that in many cases the problem of unambiguous identification of alpha lines can be overcome by implanting the fusion products that have passed the velocity filter directly into position sensitive solid state detectors. This allows to use position and time correlation methods that make a rather efficient use of parent daughter relationship for isotope identification as well as alpha branching ratio determination.

In the course of this work 29 new isotopes could be identified and a number of alpha branching ratios were measured. The fast separation has also allowed us to find two new high energy alpha lines that are emitted from high spin isomeric transitions. In a search experiment for proton radioactivity a new line of 1.19 MeV far below the energy of α lines was observed. It is very likely due to a proton decay of an isotop beyond the proton drip line. Our results are presented in Sect. 3. A discussion of the new extended Q_α systematics, partial alpha half lives, and reduced α widths together with an estimate of the character of the new high energy transitions will be given in Sect. 4. At the end of Sect. 4 we discuss our search for proton radioactivity.

2. Experimental Method

At the linear accelerator UNILAC we have irradiated targets prepared from neutron deficient isotopes of elements between Zr-Sn, Fe-Mo, and V-Ni with beams of ^{58}Ni, ^{92}Mo, and ^{107}Ag, respectively. Specific beam energies were in the range between 4.1 MeV/u and 5.9 MeV/u, average beam currents $1o^{10}$ions/s. After separation from the projectiles by the velocity filter SHIP[4]) the evaporation residues were implanted into an array of seven position sensitive silicon detectors. In the following subsections we briefly describe the velocity filter SHIP (Sect. 2.1), the implantation method (Sect. 2.2), and a newly developed position time correlation method for isotope identification and determination of half lives as well as alpha branching ratios (Sect. 2.3).

2.1 The Velocity Filter SHIP

The principle of the separation of fusion products from the projectile beam with the velocity filter SHIP

is shown in Fig. 1. A combination of two electric and four magnetic dipole fields together with two quadrupole triplets accepts radially and axially an angular range of $\pm$ 1.5^0 relative to the projectile beam axis and focusses ionic charges within a charge window of $\pm$ 1o % onto a measuring position 11 m downstream of the target position. The velocity dispersion necessary to separate projectiles and evaporation residues is large in the median plane of the ion optical system. Here a variable velocity slit allows to select a maximum velocity window of $\pm$ 5 %. The velocity dispersion in the median plane is compensated in the second symmetric half of the instrument. Two thin carbon foils of about 3o µg/cm^2, 8 cm behind the target and in front of the velocity slit are used for ion charge equilibration of the fusion products and of background projectiles, respectively.

The special transmission properties of the velocity filter result in optimal target thicknesses of about 1 mg/cm^2. Calculated total efficiencies[5]) for reactions with ^{58}Ni projectiles range from about 2o % for xn and pxn channels to about 3.5 % for αxn channels. The velocity filter is therefore partially selective for xn and pxn fusion products. The excellent selectivity from the projectile beam is illustrated in Fig. 2, which shows a typical energy spectrum obtained with a silicon surface barrier detector (45o mm^2 x 3oo µm) in the measuring position behind the velocity filter. Out of 3 x 1o^{12} projectiles only one was registered by the detector at the primary beam energy. The peak at 6o MeV corresponds to evaporation residues. The energy distribution of ^{58} Ni ions that are scattered into the velocity window of the instrument is seen to peak near 25 MeV.

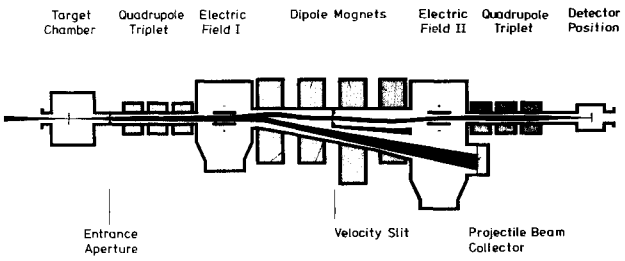

Fig. 1: Separation of evaporation residues from projectiles by the velocity filter SHIP.

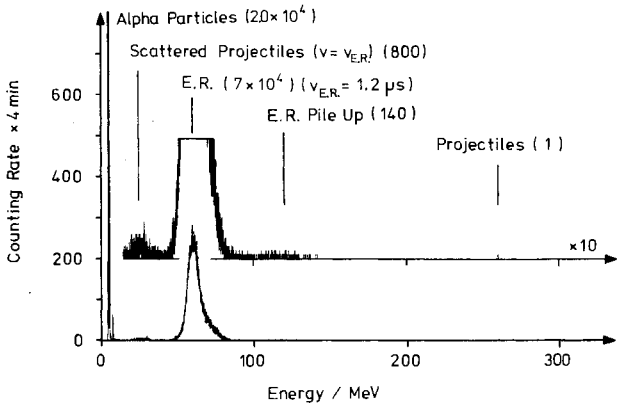

Fig. 2: Energy spectrum of implanted evaporation residues of the reaction ^{58}Ni (276 MeV)+^{103}Rh →^{161}Ta*. The number of collected particles is given in parenthesis.

2.2 The Implantation Method

The sharp peaks at the lower end of the spectrum in Fig. 2 are due to α particles from the decay of the implanted evaporation residues. The implantation depth of the fusion products with average incident energies of 6o MeV into the detector material can be estimated to be about 7 µm[6]). From a comparison with the ranges of typical α particles one can estimate that an average of 65 % of the α decays of the implanted fusion products are registered with full energy. The remaining fraction of α particles leaves the detector depositing a variable energy down to about 1.5 MeV.

The generally present small background of scattered ^{58}Ni ions was completely eleminated in the spectra by gating between UNILAC macropulses. The macroperiod of the accelerator is 2o ms with a beam pulse width of about 4 ms. The complexity of the alpha spectra obtained in most reactions is illustrated in Fig. 3.

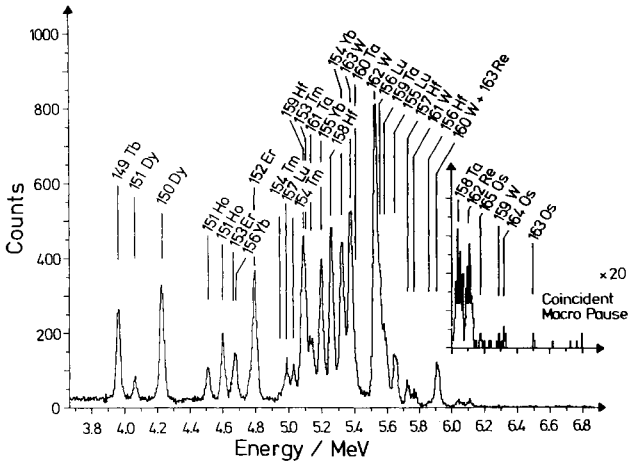

Fig. 3: α singles spectra of implanted evaporation residues taken during the irradiation of a ^{110}Cd target with 319MeV ^{58}Ni projectiles. All α lines could be identified.

With a 3oo mm^2 surface barrier detector, cooled down to -15^{0}C, it was possible to achieve a resolution of 17 keV at FWHM. We conclude that the implantation method combines the advantages of high geometrical efficiency with excellent resolution.

The implantation method requires special care with the energy calibration, since the detector also registers the recoiling daughter nuclei. Typical recoil energies are 15o keV, roughly half of which is converted into electron hole pairs giving rise to increased alpha signals as compared to signals from external alpha sources. The calibration was therefore made internally using six known alpha emitters identified in the on-line spectra. The corresponding energies are tagged with the superscript b in Table 1, column 2. This method assumes that the registered recoil energy is proportional to the alpha energy. A linear least squares fit to the six known alpha energies resulted in standard deviations of less than 5 keV.

2.3 Isotope Identification, Half Life, and Alpha Branching Ratio Determination: A new Position and Time Correlation Method

Unambiguous identification of new alpha lines is

best performed in establishing decay chains leading to known transitions. A technique of position and time correlation measurements between subsequent decay signals was developed. The evaporation residues were implanted into an array of seven position sensitive silicon detectors each with a width of 9 mm and a height of 27 mm (Fig. 4).

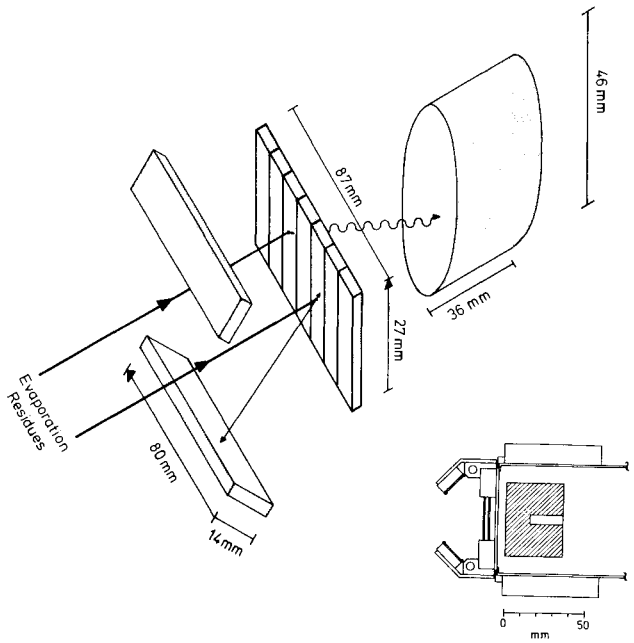

Fig. 4: Detector system for identification of rare isotopes.

Energy, time, detector number, and position of implantation of the incident evaporation residues and of the emitted α particles were measured and stored in list mode on magnetic tape.

The position resolution of the solid state detectors was 21o μm (FWHM). This is large compared to the range, 7 μm at 6o MeV[6]), of the implanted fusion products, their very small estimated recoil path, o.4 μm, after alpha emission, and typical ranges of the alpha particles themselves, (25-4o)μm.

Our identification method is based on the fact that for any incident nucleus its subsequent chain of decays must be observed at its position of implantation within a time window determined by the half lives of the isotopes. Unambiguous identification of new α lines is best performed, if a correlation to known transitions can be established. Such correlations can easily be determined from two dimensional plots of parent energies on the ordinate and of daughter energies, following within a certain time window and a position window relative to the parent position, on the abscissa. An example of such a plot is shown in Fig. 5.

True correlations can be found easily by an accumulation of events. Analyzing projected spectra onto the energy axis obtained with additional energy windows, positions and intensities of correlated events can be measured very accurately even in cases of unresolved lines in complicated singles spectra.

It immediately follows from the above observations that the correlation method allows to measure α branching ratios with good precision. Half lives are obtained by investigating the time differences of correlated events.

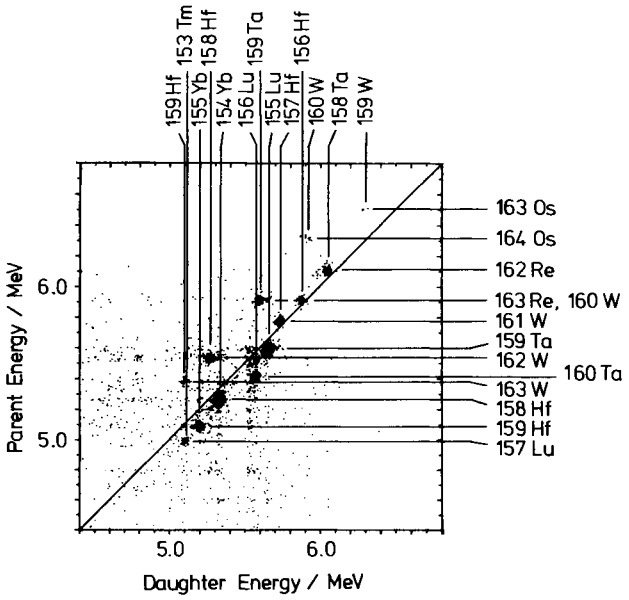

Fig. 5a: α-α coincidence spectrum.
Reaction: $^{58}Ni + ^{110}Cd \rightarrow ^{168}Os(E^{*} = 83$ MeV)
Time window: 2oo ms
Position window: ± 45o μm

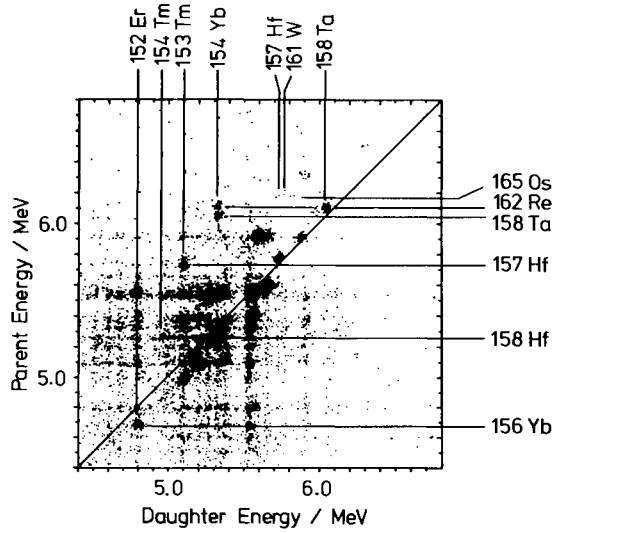

Fig. 5b: α-α coincidence spectrum.
Reaction: same as above
Time window: 8.2 sec
Position window: ± 15o μm

For investigation of coincident γ or x-rays we put a 12 % efficiency γ-x detector just behind the array of particle detectors. We also mounted two additional Si-detectors looking into the backward direction to measure some of those particles leaving the detector array.

3. Results

In the course of this work 22 new α emitters could be identified. Six new ß emitters were identified by α-(ß-ß-)α correlations. A compilation of all

new isotopes with energies, halflives, and branching ratios is given in Table 1. New data on previously known isotopes are also listed. In many cases uncertainties in the values could be reduced.

Since the analysis of the data was straight forward in many cases but has to be discussed carefully in detail we refer to our previous publications (Ref. 7, 8). In this paper we will describe in more detail the identification of two α emitting isomeric states and the discovery of a new low energetic line in the particle spectra.

3.1 Two new alpha unstable high spin isomers

Two short lived high energy transitions - denoted with α_1 and α_2 in Fig. 6 - were observed in various reactions. Fig. 7 shows all investigated compound systems where we found these lines.

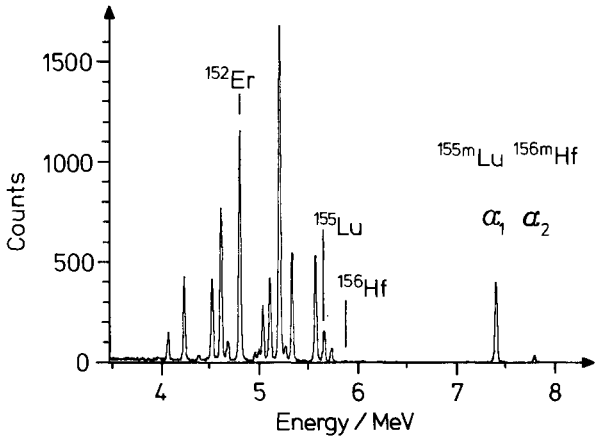

Fig. 6: α spectrum taken during the irradiation of ^{102}Pd with ^{58}Ni at excitation energies of the compound nucleus ^{160}W of 7o MeV.

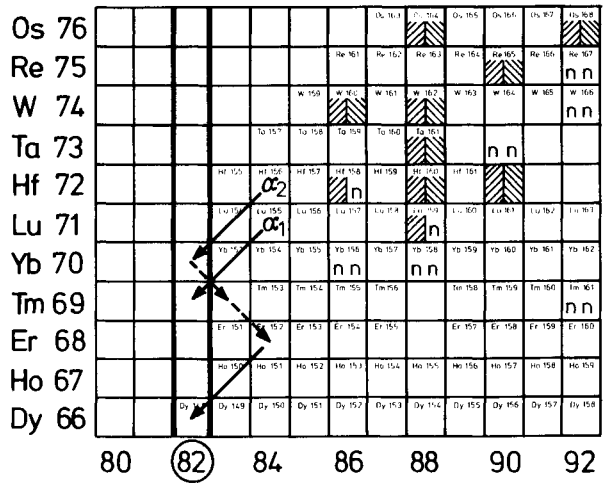

Fig. 7: Chart of nuclei with investigated compound nuclei. α_1 observed: ▨; α_2 observed: ▩; no high energetic α line observed: "n".

The excitation energies of the compound nuclei were in the region between 4o MeV and 9o MeV. The highest measured cross section for the line α_1 was 1.1 mb in the reaction ^{58}Ni + ^{102}Ru → ^{160}Hf(E^* = 72 MeV) and for the line α_2 it was o.26 mb in the reaction ^{58}Ni + ^{102}Pd → ^{160}W(E^* = 57 MeV). The half life of (2.6o ± o.o7)ms for the line α_1 was calculated by fitting an exponential decay function to the intensity during the beam pulses (Fig. 8a). A time correlation analysis between evaporation residue signals and alpha particle signals gave the half life (444 ± 17)μs for the line α_2 (Fig. 8b).

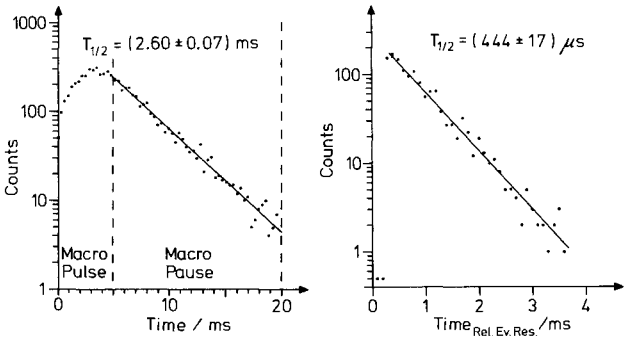

Fig. 8a,b.: Decay curves of the lines α_1 (a) and α_2 (b).

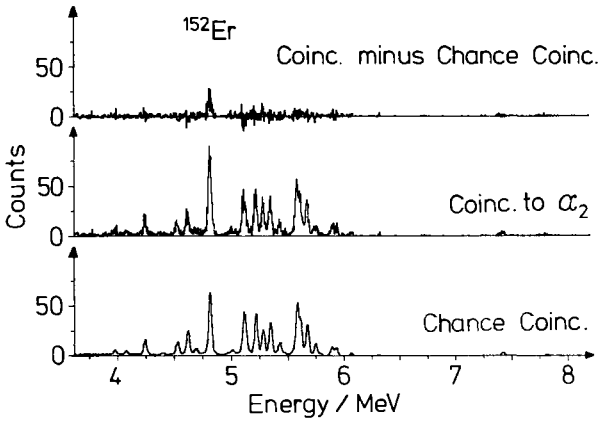

Fig. 9: Position-time coincidence spectrum to the high energetic line α_2.
Time window: 32 sec
Position window: ± o.6 mm

For this higher energetic line α correlation was found to the α decay of ^{152}Er (Fig. 9). Therefore, possible emitters of α_2 are the isobars A = 156. From those the isobars ^{156}Lu and ^{156}Yb can be excluded, because α_2 was not observed in reactions leading to ^{159}Lu as compound nucleus at excitation energies of 57, 61, and 68 MeV. The only possible decay chain left is drawn in Fig. 7 and starts from the isotope ^{156}Hf identified as emitter of α_2.

A correlation of α_1 with daughter α lines could not be observed. The reactions leading to ^{159}Lu as compound nucleus show that one of the isotopes ^{155}Lu or ^{156}Lu is the emitter. From these two ^{156}Lu can be excluded because in this case a correlation with ^{152}Er would have been observed like in the former

Table 1: Summary of α decay measurements and comparison with calculated α und β partial half lives

Isotope	E_α/keV	$T_{1/2}$ exp.	b_α/% exp.	b_α/% theor.[f]	$T_{1/2,\alpha}$ calc.	$T_{1/2,\beta}$ theor./18/	$\frac{W_\alpha, \Delta l=0}{W_\alpha(^{212}Po)}$
$^{171}Pt^x$	6448 ± 5	> 2o ms		97	58 ms	1.6 s	< 3,o [g]
$^{170}Pt^x$	6545 ± 8	$(6\ ^{+5}_{-2})$ ms		98	27 ms	1.1 s	$4.5\ ^{+2.7}_{-2.2}$ [g]
$^{169}Pt^x$	6678 ± 15	$(2.5\ ^{+2.5}_{-1.o})$ ms		99	9.5 ms	o.8 s	$3.8\ ^{+3.3}_{-2.1}$ [g]
$^{168}Pt^x$	6824 ± 2o			1oo	3.2 ms	o.9 s	-
$^{167}Ir^x$	6386 ± 1o	> 5 ms		95	41 ms	o.8 s	< 9 [g]
$^{166}Ir^x$	6541 ± 2o	> 5 ms		99	12 ms	o.8 s	< 2.8 [g]
^{167}Os	5836 ± 5	(1.o5 ± o.35)s	58 ± 12[x]	56	2.o s	2.5 s	1.1 ± o.4
^{166}Os	5981 ± 6	(181 ± 38)ms	72 ± 13[x]	82	54o ms	2.5 s	2.15 ± o.61
^{165}Os	6164 ± 1o	$(65\ ^{+7o}_{-3o})$ ms[x]	1oo ± 4o[x]	92	11o ms	1.2 s	$1.6\ ^{+1.7}_{-o.9}$ [g]
$^{164}Os^x$	632o ± 2o	(41 ± 2o)ms	1oo ± 7o	98	29 ms	1.6 s	$o.71\ ^{+o.94}_{-o.3o}$ [g]
$^{163}Os^x$	651o ± 3o			99	6.3 ms	o.8 s	-
$^{165}Re^x$	55o6 ± 1o	(2.4 ± o.6)s	13 ± 3	14	19 s	3.1 s	1.o5 ± o.38
$^{164}Re^x$	5778 ± 1o	(o.88 ± o,24)s		58	1.3 s	1.8 s	-
$^{163}Re^x$	5918 ± 6	(26o ± 4o)ms	64 ± 18	78	36o ms	1.3 s	o.92 ± o.3o
$^{162}Re^x$	6119 ± 6	(1oo ± 3o)ms	> 3	94	61 ms	1.o s	o,63 ± o.2o[g]
$^{161}Re^x$	6279 ± 1o	$(1o\ ^{+\ 15}_{-\ \ 5})$ ms	> 1	99	16 ms	1.1 s	$1.67\ ^{+2.o}_{-1.1}$ [g]
^{166}W	4733 ± 1o[c]	(16 ± 3)s[e]	o.6 ± o.2[x]	o.o5	44 ks	2o s	16 ± 6.5
^{165}W	49o2 ± 2o[c]	(5.1 ± o.5)s[e]	< 1.5 [x]	o.15	5.4 ks	8 s	< 22
^{164}W	5148 ± 5[b]	(6.4 ± o.8)s[c]	2.6 ± 1.7[x]	2.5	31o s	8 s	1.24 ± o.83
^{163}W	5384 ± 5[b]	(3.o ± o.2)s[c]	41 ± 5[c]	14	24 s	4 s	3.27 ± o.49
^{162}W	5538 ± 5[c]	(139o ± 4o)ms[x]	46 ± 4[x]	44	5.o s	4 s	1.67 ± o.18
^{161}W	5777 ± 5[c]	(41o ± 4o)ms[x]	82 ± 26[x]	8o	49o ms	2 s	1.o2 ± o.34
$^{160}W^x$	592o ± 1o	(81 ± 15)ms	94 ± 4o[x]	95	14o ms	2.5 s	1.73 ± o.36[g]
$^{159}W^x$	6299 ± 6	(7.3 ± 2.7)ms	2oo ± 12o	1oo	5.5 ms	1.2 s	o.75 ± o.37[g]
$^{158}W^x$	645o ± 3o			1oo	1.7 ms	o.8 s	-
$^{161}Ta^x$	5148 ± 5			5	1oo s	5.5 s	-
$^{160}Ta^x$	5413 ± 5			34	6.2 s	3.2 s	-
$^{159}Ta^x$	56o1 ± 6	(57o ± 18o)ms	8o ± 5	77	97o ms	3.2 s	1.39 ± o.46
$^{158}Ta^x$	6o51 ± 6	(36.8 ± 1.6)ms	93 ± 6	99	16 ms	2.3 s	o.41 ± o.o4
$^{157}Ta^x$	6219 ± 1o	(5.3 ± 1.8)ms	1oo ± 23	1oo	3.9 ms	1.3 s	o.77 ± o.27[g]

Isotop	E_α/keV	$T_{1/2}$ exp.	b_α/% exp.	b_α/% theor.[f]	$T_{1/2,\alpha}$ calc.	$T_{1/2,\beta}$ theor./18/	$W_\alpha, \Delta l=0$ / $W_\alpha(^{212}Po)$
^{160}Hf	4777 ± 5[c]	12 s[e]	2.3 ± o.6[c]	o.5	2.6 ks	13 s	4.8 ± o.3
^{159}Hf	5o95 ± 5[c]	(5.6 ± o.5)s[e]	12 ± 1[c]	11	62 s	8 s	1.33 ± o.18
^{158}Hf	5268 ± 5[b]	(3.2 ± o.6)s[c]	46 ± 3[x]	39	9.8 s	6.2 s	1.41 ± o.29
^{157}Hf	5735 ± 5[d]	(11o ± 6)ms[c]	91 ± 7[x]	98	96 ms	5 s	o.82 ± o.o9
$^{156}Hf^x$	5878 ± 1o	(25 ± 4)ms	1oo ± 19	99	27 ms	3.2 s	1.12 ± o.21[g]
$^{156m}Hf^x$	78o4 ± 15	(444 ± 17)µs			32 ns	-	(72±7)·1o^{-6} [g]
$^{155}Hf^x$	477o[a]	(o.89 ± o.12)s		o.o6	3,3 ks	2 s	-
$^{154}Hf^x$	365o[a]	(2 ± 1)s		2·1o^{-9}	85 Gs	1.6 s	-
^{157}Lu	4996 ± 5[c]	(4.5 ± 1.5)s[e]	6 ± 2[x]	14	62 s	1o s	o.83 ± o.39
^{156}Lu	545o ± 1o[c]	∿ o.5 s[e]		95	o.51 s	8 s	1.o5[g]
^{156}Lu	5568 ± 5[c]	(18o ± 2o)ms[c]	1oo ± 25[x]	98	16o ms	8 s	o.92 ± o.11[g]
^{155}Lu	5656 ± 6[c]	(7o ± 6)ms[c]	79 ± 4[x]	99	73 ms	6.2 s	o.85 ± o.1o
$^{155m}Lu^x$	74o8 ± 1o	(2.6o ± o.o7)ms		-	14o ns	-	(55 ± 4)·1o^{-6}g
$^{154}Lu^x$	453o[a]	(o.96 ± o.1o)s		o.o24	21 ks	5 s	-
$^{153}Lu^x$	346o[a]			3·1o^{-10}	75o Gs	2 s	-
^{158}Yb	4o69 ± 1o[e]	(99 ± 12)s[e]	< o.9[x]	o.oo3	3.3 Ms	1oo s	< 4oo
^{157}Yb	45o5 ± 1o[c]	(38.6 ± 1.o)s[e]		o.4	7.4 ks	32 s	-
^{156}Yb	4686 ± 1o[c]	(24 ± 1)s[e]	21 ± 6[x]	4	75o s	32 s	6.5 ± 2.o
^{155}Yb	52o6 ± 5[c]	(1.59 ± o.22)s[c]	84 ± 1o[x]	9o	2.1 s	18 s	1.o9 ± o.21
^{154}Yb	5332 ± 5[c]	(41o ± 3o)ms[c]	93 ± 2[x]	97	58o s	2o s	1.34 ± o,12
^{153}Yb	419o[a]			o.oo14	66o ks	9 s	-
$^{152}Yb^x$	312o[a]			3·1o^{-12}	23o Ts	6 s	-
^{154}Tm	4959 ± 5[c]	(5 ± 1)s[e]	44 ± 15	72	9.6 s	25 s	o.84 ± o.33
^{154}Tm	5o35 ± 5[c]	(3.5 ± o.1)s[e]		86	4.1 s	25 s	-
^{153}Tm	51o9 ± 5[c]	(1.58 ± o.15)s[e]	95 $^{+5c}_{-8}$	94	1.9 s	32 s	1.29 ± o.17
$^{152}Tm^x$	399o[a]			5·1o^{-4}	3.5 Ms	16 s	-
^{153}Er	4674 ± 1o[c]	(36 ± 1)s[e]	53 ± 3[e]	56	8o s	1oo s	1.15 ± o.16
^{152}Er	48o2 ± 5[b]	(9.8 ± o.3)s[e]	93 ± 4[c]	86	18 s	11o s	1.71 ± o.13
^{151}Ho	4519 ± 5[c]	(35.6 ± o.4)s[e]	18 ± 5[e]	56	16o s	2oo s	o.8o ± o.23
^{151}Ho	46o6 ± 5[b]	(47 ± 2)s[e]	13 ± 4[e]	78	55 s	2oo s	o.15 ± o.o5
^{151}Dy	4o68 ± 1o[c]	(1o8o ± 12)s[e]	5.9 ± o.6[e]	5	19 ks	1.o ks	o.96 ± o.18
^{150}Dy	4232 ± 5[b]	(43o.2 ± 1.2)s[e]	38 ± 5[c]	34	1.9 ks	1.o ks	1.63 ± o.24
^{149}Tb	3963 ± 1o[c]	(14.6 ± o.3)ks[e]	16 ± 4[e]	5	24 ks	1.3 ks	o.24 ± o.o7

References to Table 1:

[x] New isotopes, new isomeric state or new decay data

[a] Extrapolated value determined with data from Ref. 9

[b] The following literature values were used for energy calibration: ^{150}Dy: (4,233±4) keV (1σ); ^{151}Ho: (4,607±3) keV (11); ^{152}Er: (4,799 ± 3) keV (11); ^{158}Hf: (5,270±1σ) keV (12); ^{163}W: (5,385±5) keV (13); ^{164}W: (5,150±5) keV, mean value of Ref. (13) and Ref. (14)

[c] Value agrees with literature (15,16,17); errors could be reduced in many cases

[d] Value differs significantly from literature (17)

[e] Literature value (11,15,17); not measured in present work

[f] $b_{\alpha exp} = I_{\alpha,daughter}/I_{\alpha,parent}$ from α intensity ratios, $b_{\alpha theor} = T_\beta/(T_\alpha + T_\beta)$ from theoretical α and β half lives

[g] calculated with b_α = 100 %

discussion of α_2. We conclude ^{155}Lu is the emitter of α_1.

3.2 Proton radioactivity of the new isotope ^{151}Lu

In a search experiment for proton unstable isotopes we have investigated a variety of compound systems near the proton drip line. With beams of ^{58}Ni and ^{92}Mo we could produce the most neutron deficient compound nuclei between the elements Er and Bi that can be produced with stable targets.

In one of these reactions, ^{58}Ni + ^{96}Ru → ^{154} Hf, we observed a line of low intensity far below the energies of the α lines (Fig. 1σ). This spectrum was taken with a 3σσ μm thick Si detector. Fig. 11 shows a spectrum taken with a 14σ μm thick detector. Here the background of electrons and ß particles is highly reduced and the new line is observed in a nearly background free part of the spectrum. The distribution of events between channel numbers 8σσ and 19σσ is due to α particles leaving the detector in backward direction.

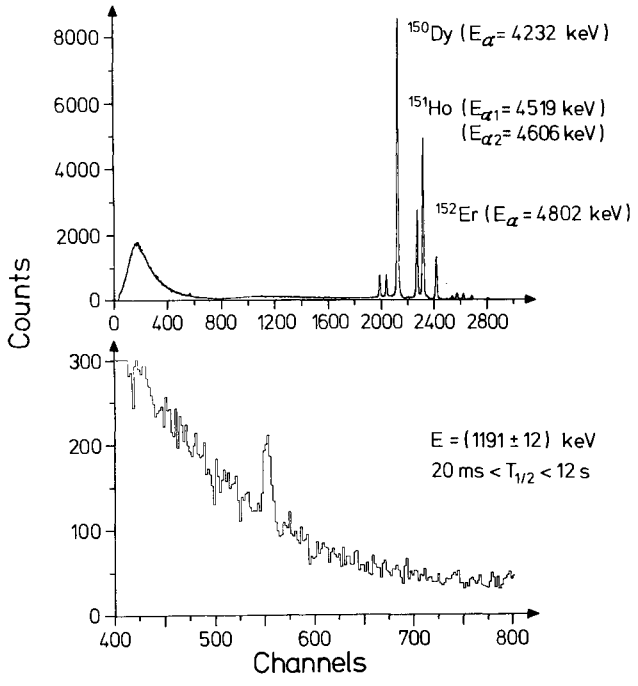

Fig. 1σ: Energy spectrum taken with a 3σσ μm thick Si detector (bin size of channels: 2) Reaction: ^{58}Ni + ^{96}Ru → ^{154}Hf (E^*=47 and 54 MeV).

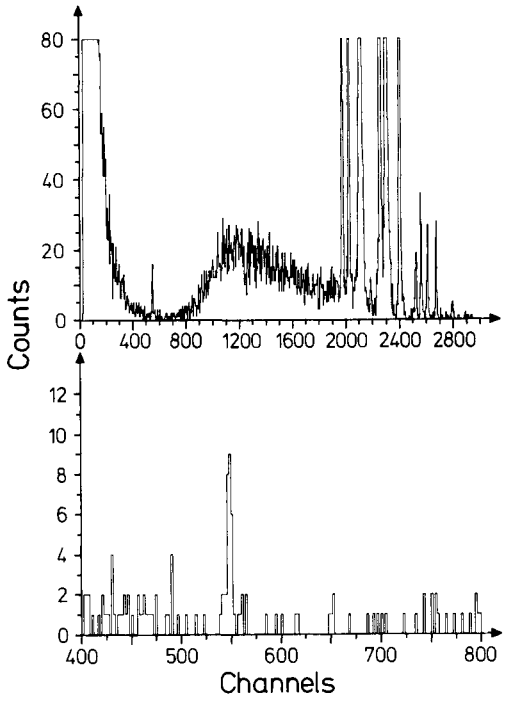

Fig. 11: Energy spectrum taken with a 14σ μm thick Si detector (bin size of channels: upper part 4, lower part 2) Reaction: see Fig. 1σ

Excitation functions were measured for the 1.19 MeV line and the A = 152, 151, and 15o isobars, produced in 2, 3 and 4 nucleon evaporation channels (Fig. 12). The statistical errors of the cross sections are of the order of the point size. Systematic errors due to calculated efficiencies can shift the data points by a factor of 2.

We see from the figure that the curve of the 1.19 MeV line is well below the ^{151}Ho curve indicating a three nucleon evaporation except a small shift towards higher energies. Such a shift is also observed in the compound system $^{160}W^{*}$ between the 2pn and p2n evaporation channels (Fig. 12).

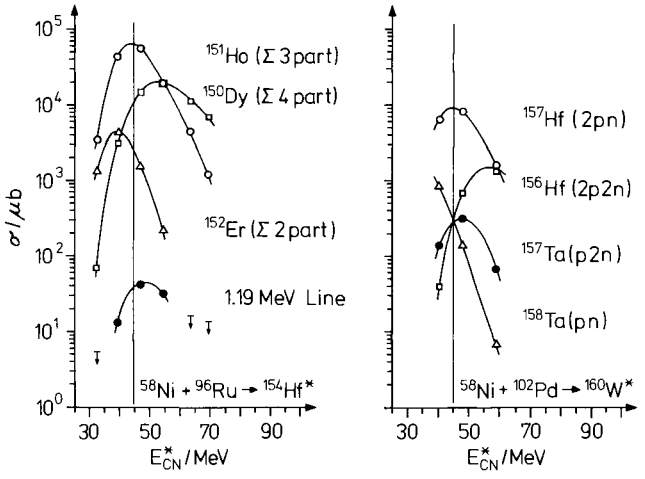

Fig. 12a,b: Excitation functions of α lines and the new 1.19 MeV line in the reaction ^{58}Ni + ^{96}Ru (a) compared to excitation functions of α lines in the reaction ^{58}Ni + ^{102}Pd (b).
The vertical line of 45 MeV is drawn near the maximum of the 3 particle evaporation channel to guide the eye.

A qualitative explanation of this shift lies in the slightly larger average excitation energy removed by neutrons as compared to protons in these very proton rich nuclei. We can therefore argue that the emitter of the 1.19 MeV line is very likely an A = 151 isobar.

To get information about the character of the radiation we can compare the intensity ratios of the new line to an appropriate α line calculated for the thick and for the thin detector. These ratios are independent of detector thicknesses, whenever both particles cannot penetrate the detector. This is the case for low energetic α particles ($R_{\alpha,E=5\ MeV}$=3o μm) and protons ($R_{p,E=1.2\ MeV}$=22 μm, Ref. 6). For electrons $R_{e,E=1.2\ MeV}$=2.4 mm) the intensity normalized to α particle intensities is proportional to the detector thickness d for values of d << R_e. For our detectors we calculate a ratio $(I_e/I_\alpha)_{3oo\ \mu m}/(I_e/I_\alpha)_{14o\ \mu m}$ = 2.14. This value is reduced to 1.77 when corrected for losses of electrons at the detector borders. Not included are losses of electrons due to scattering. This effect has more influence on the thin detector and will again increase the above value.

Our measured intensity ratio for the 1.19 MeV line normalized to ^{152}Er α particle intensities is 1.o7 ± o.19. This value is 3.7 error bars below the value expected for electrons, but overlaps with those expected for protons.

We therefore preliminarily assign the new 1.19 MeV line to proton decay of an isotope resulting from a three particle decay channel. Although the experiment has not allowed us so far to determine unambiguously the nuclear charge of the emitter, a number of systematics considerations tend to strongly favour the isotope ^{151}Lu (resulting from the p2n de-excitation channel) as the parent nucleus for this proton radioactivity. This will be taken up in detail in the discussion (sect. 4).

For the half live of the 1.19 MeV transition we could measure lower and upper limits. A decrease of the intensity was not observed during the 15 ms beam pauses within statistical errors giving a lower limit of 2o ms < $T_{1/2}$. The thin detector was moved every 7oo seconds for a period of 1oo seconds into the separated beam of evaporation residues. The line could only be observed during the irradiations leading to an upper limit of 12s > $T_{1/2}$.

4. Discussion

4.1 Q_α-Values, α and ß decay Probabilities

The data on the new alpha emitters identified in this work allow to broaden the Q_α systematics as is shown in Fig. 13. The alpha energies for the 22 new isotopes fit well into the general trend set by previously known alpha emitters. Since most of the isotopes investigated are very far from the stability line their α decay energies allow a stringent test of the various mass calculation schemes. A comparison of experimental and theoretical α energies is shown in Fig. 14 for the lightest known isotopes of Hf, Ta, W, and Re.

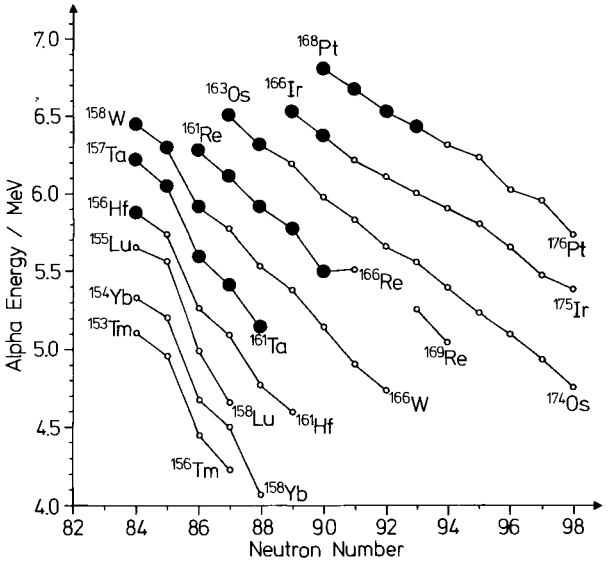

Fig. 13: Alpha systematics of neutron deficient isotopes of elements from Tm to Pt. The new isotopes are marked as bigger dots. They fit very well into the systematics of the previously known isotopes.

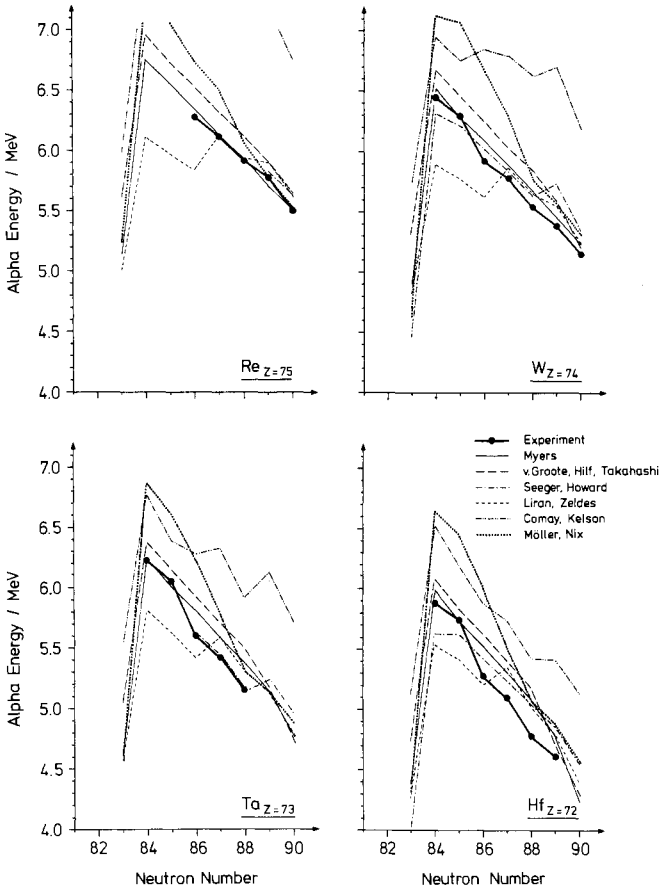

Fig. 14: Comparison of α energies of Re, W, Ta, and Hf isotopes near the closed neutron shell N = 82 with predictions of six different mass tables (19,2o).

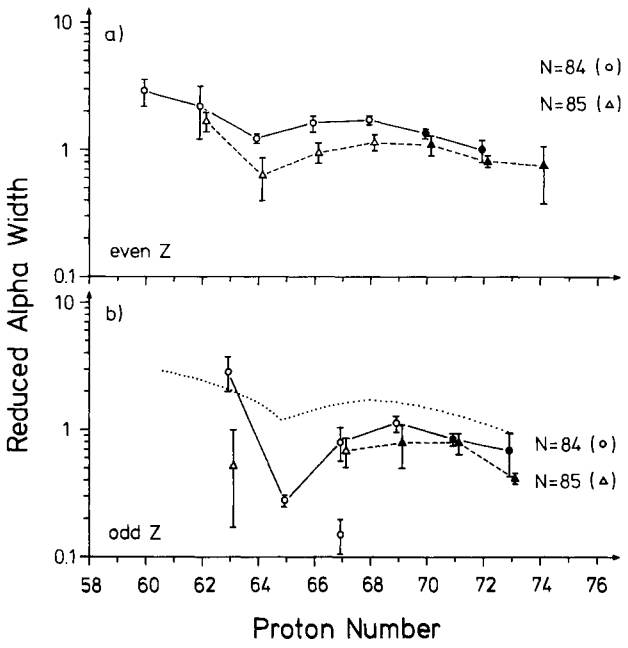

Fig. 15: Reduced α widths of N = 84 and 85 isotopes as function of the proton number. For isotones marked with filled symbols newly measured α branchings, half lives, or energies were used.

A number of short comments can be made: 1) from Fig. 14 it appears that Myers' droplet approach gives a particularly good account of the experimental data, with deviations < o.25 MeV; 2) the striking discontinuity in Fig. 13 at the neutron numbers 84-86, which is very stable against the variation of the nuclear charge, is not reproduced by any of the mass calculation schemes shown in Fig. 14; for the approaches of v. Groote et al. and of Myers, which use a simple semiempirical Ansatz for the shell correction term, this deficiency is not unexpected; 3) the calculations of Möller and Nix which determine the shell correction "microscopically", tend to reproduce correctly the heavier isotopes (N = 88-9o), but show an increasing deviation from the data as the N = 82 shell is approached; this strongly indicates an overestimate of the N = 82 shell strength in this particular calculation; the data tend to favour a rapid change of the shell correction until N = 86, but for greater neutron numbers the change is more gradual.

In order to show the dependence of α decay probabilities on nuclear structure, we have drawn in Fig. 15 the reduced α widths, w_α, as function of the proton number over a wide range from Z = 6o to Z = 74, separately for the neutron number N = 84 and 85.

The reduced α widths $w_\alpha \sim \lambda_\alpha / P$ were calculated with the barrier penetrabilities P and the partial α decay constant λ_α ($\lambda_\alpha = b_\alpha \cdot \ln 2 / T_{1/2}$, b_α is the α branching ratio and $T_{1/2}$ is the total half life).

The barrier penetrability was calculated with a WKB method[21]). As experimental input values we used the values given in Table 1 and for the elements Neodymium to Erbium the values given in Ref. 22 to Ref. 29. The errors were determined by the compounded uncertainties of the experimental branching ratios, half lives, and Q_α-values. All reduced widths were calculated assuming s-wave α particles and were normalized to the reduced width of the ^{212}Po ground state transition.

Reduced widths with the smallest experimental errors are available for the N = 84 isotones, Fig. 15a. Theoretical calculations of Macfarlane et al.[30]) for the N = 84 isotones, with BCS wave functions and pure shell model wave functions show, in agreement with the experimental data, a dip of the α widths at the sub-shell Z = 64. In filling the $\pi h_{11/2}$ sub-shell the calculated widths run through a mid-shell maximum at Z = 7o-72, whereas the experimental data show a maximum at Z = 68. Possibly, the reason for the earlier decrease of the α widths are strong admixtures of the $\pi d_{3/2}$ shell. For this subshell relatively small widths were calculated[30]).

The dashed curve in Fig. 15a connects the widths of the odd N = 85 isotones. These values show the same dependence as function of the proton number, but are in general 2o % to 4o % lower. This indicates that for the N = 85 isotones s-wave α particle decay is most likely with configurations very similar to those involved in the even-even isotones, except for a moderate odd particle blocking effect[31]). The full line connecting the odd Z, N = 84 isotones of Fig. 15b is, except for a shift of one unit on the proton number scale very similar to the dashed line, Fig. 15a. We conclude that the odd proton blocking effect on the α widths is similar in magnitude to the odd (N = 85) neutron blocking. Finally, we note that the α widths of all odd-odd nuclei (dashed line, Fig. 15b) are on the average about 3o % lower than the α widths of the odd-even and even-odd nuclei.

Assuming a reduced α width of one we have calculated partial α half lives which are listed in columns 6 of Table 1. Predictions are given for the unknown α half lives and may be off by about 3o %, corresponding to the variation of the reduced α widths.

Theoretical ß half lives taken from calculations with the gross theory of ß decay of Takahashi et al.[18]) are listed in column 7 of Table 1. These values imply a Gaussian ß strength function and allow for the occurrance of transitions to low lying states. They differ from the experimental values on the average by only 4o %. Therefore, the theoretical ß half lives were used together with the theoretical α half lives to calculate α branchings using the expression $b_\alpha = T_\beta/(T_\alpha + T_\beta)$. These values are presented in column 5 of Table 1.

4.2 High Spin Isomers

The measured energies and half lives of the high energy transitions in ^{155}Lu and ^{156}Hf allow us to estimate reduced alpha widths assuming that the alpha branching ratio is 1. This is summarized in Table 2. One finds a rather strong hindrance of about $1o^5$ if one assumes s-wave alpha decay, an indication of a possible high spin isomerism. One obtains reduced widths closer to 1, again relative to the ^{212}Po ground state decay, if one assumes an angular momentum change of (1o±2)ħ (Table 2). The difference in the Q_α values between high energy transitions and ground state transitions give the excitation energies of the isomeric states of (1798 ± 12) keV and (1977 ± 18) keV in ^{155}Lu and ^{156}Hf, respectively.

It is interesting to note in this context that a number of isomers in this energy range have been found for proton rich nuclei near the N = 82 shell in reactions with α and ^{16}O beams. Broda et al.[32]) report on a positive parity state in ^{147}Gd at 176 MeV with spin 21/2 ħ. A o.5 µs isomer was found by Daly et al.[33]) in ^{148}Dy at 2.92 MeV with a spin of 1o ħ. These isomers have been explained in terms of shell model configurations[32]) in the vicinity of ^{146}Gd, which is interpreted as a doubly closed shell configuration[40]). Finally, we add that the two states belong to isotones with N = 84. The systematics of reduced α widths shows that these isotones two neutrons beyond the closed shell have an enhanced ground state transition probability. This may explain that especially for these isotones α decay becomes a competitive decay mode of isomeric states.

Table 2: Comparison of the half lives of the two high energetic α lines with calculations for different changes in angular momentum. The calculations for Δl=0 show the hindrance of a decay by a factor of about $1o^5$ in both cases.

	E_α/keV	$T_{1/2,exp.}$	E_α/keV	$T_{1/2,exp.}$
	7,4o8±1o	(2.6o±o.o7) ms	7,8o4±15	(444±17) µs

$\Delta l_\alpha/h$	W_α	$T_{1/2,theory}$	W_α	$T_{1/2,theory}$
o	$2\cdot1o^{-5}$	6o ns	$1\cdot1o^{-5}$	6 ns
8	o.o2	5o µs	o.o1	5 µs
1o	o.6	1.7 ms	o.3	o.16 ms
12	38o	1oo ms	17o	9 ms

4.3 Proton Radioactivity

The possibility to measure proton radioactivity for many neutron deficient isotopes is pointed out by Goldanskii[35]). Promising experiments are proposed for nuclei with Z > 5o. For lighter nuclei proton decay from isomeric states is also considered. Such a transition was observed 197o by Jackson et al.[36]) for a ^{53m}Co isomer. For heavier systems only ß delayed proton emission is known. A review is given by J. Hardy[37]).

In our experiment we have preliminarily assigned the observed 1.19 MeV line to ^{151}Lu (Z=71, N=8o). One of our prime motivations for searching in this mass and Z region was the expected absence of α emission as a competitive decay mode. So far no α emitters with Z > 6o and N < 84 are known, a fact that can be understood by the strong reduction in the Q_α values when crossing the N = 82 shell starting from heavier isotopes (N ≥ 84).

Before coming back to a more detailed discussion of the observed transition in terms of a proton radioactivity, let us give other arguments against the possibility of a conversion electron line in addition to the detector response argument given already in section 3. If the observed transition was due to electron conversion, then compatibility with the measured half-life limit would e.g. require an M4 transition. We observe no L conversion line in the particle spectra (in addition to the K conversion line). The L line would be expected with 2o % of the intensity of the K-line at channel number 575 in the spectra of Fig. 1o and 11. In addition no strong γ line is observed at the corresponding energy. Such a line would be expected from a calculated conversion coefficient of 3 % for an M4 transition.

Although we plan further experiments to confirm our present assignment, a number of considerations can be given already now, that support ^{151}Lu as the most likely proton emitter if ground state to ground state decay is assumed. Of all the possible three particle emission channels to which we have shown the activity to belong (section 3) from the excitation function studies, ^{151}Lu is the isotope with the most loosely bound proton. This general conclusion is common to all mass calculations, despite the fact that they may differ considerably in the exact value of the predicted Q_p value.

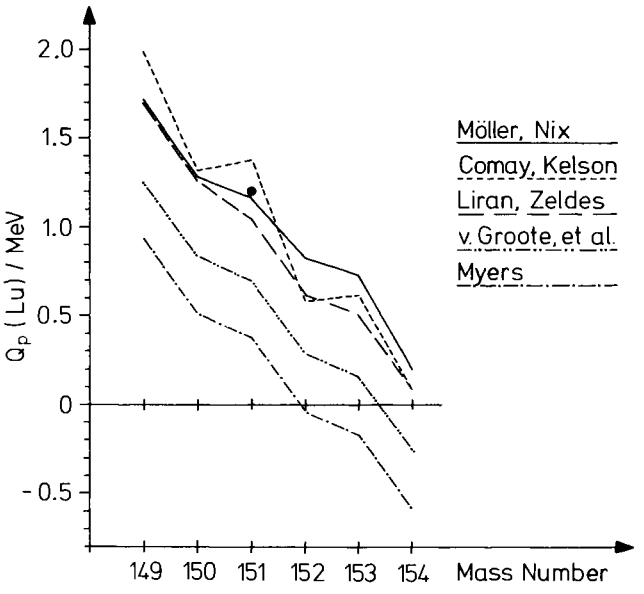

Fig. 16: Comparison of the Q_p value of ^{151}Lu with predictions of five different mass tables (19, 20).

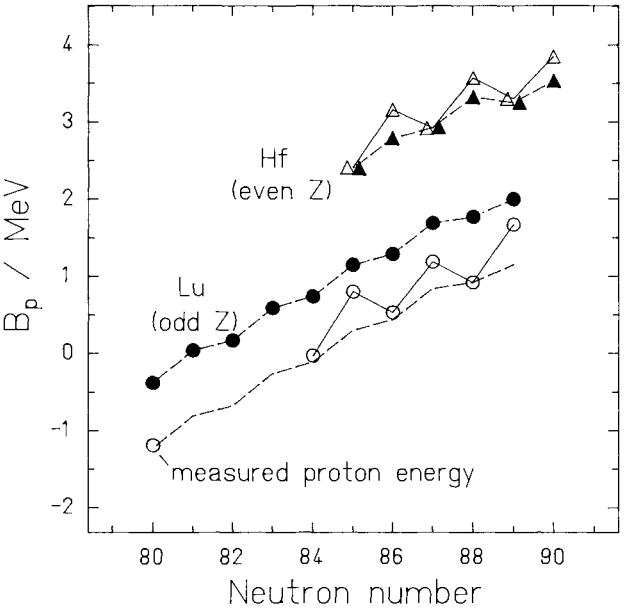

Fig. 17: Proton separation energies of Hf and Lu isotopes. See text for comments.

In Fig. 16 we have compared calculated Q_p values for Lu isotopes with the measured value assuming its assignment to mass 151. Three groups of authors, Möller and Nix, Comay and Kelson, Liran and Zeldes[19,20] predict values rather close to the measured point. The prediction of Myers lies however as much as 800 keV too low. This is rather intriguing since the droplet approach was shown in Fig. 14 to be in excellent agreement with Q_α systematics. In order to understand this apparent discrepancy we have checked the performance of Myers' droplet formula for heavier Hf and Lu isotopes where the proton binding energies Bp are known[9]. This is shown in Fig. 17 as a function of the neutron number. Full symbols represent the calculation[38], open symbols stand for experimental data. From this figure it is apparent that the calculation has problems with the pairing energy. It both underestimates the proton-proton pairing energy (systematic difference between Hf and Lu isotopes) and the proton-neutron pairing energy which is very apparent from the odd-even staggering of the straight lines joining the data. Although the calculation is in excellent agreement with the data for odd neutron Hf isotopes it systematically overestimates by about 0.8 MeV the proton separation energy of the even neutron Lu isotopes. ^{151}Lu (N = 80) belongs into this category. The lowest dashed line in the figure simply represents Myers' calculations for Lu shifted downward by 0.8 MeV so that it agrees with the Bp values of ^{155,157,159}Lu. This line goes almost exactly through the measured proton energy. Thus our measured value appears to be in rather good agreement with what we can reasonably extrapolate from known ground state Q_p values at the present time.

It is interesting to speculate about the reasons for the enhanced pairing effects implied by the data as compared to the global Ansatz of Myers[38]. This could be due to the availability at, or close to, the Fermi surface of single particle orbits with the same high angular momenta, i.e. high degeneracy, a feature which tends to enhance pairing: the Lu and Hf isotopes are in the $\pi h_{11/2}$ proton subshell; for N > 82 a strong pn pairing could result from the coupling to $h_{9/2}$ neutron particle states and this coupling could be replaced for N < 82 by $(h_{11/2})^{-1}$ neutron hole states. This would justify the continuation of the odd-even staggering of Bp down to ^{151}Lu.

The possible dominance of high orbital angular momenta could also explain the relatively long half-life observed. Emission of a proton from the $\pi h_{11/2}$ subshell in ^{151}Lu to the (spin zero) ground state of ^{150}Yb would involve an angular momentum change of 5 $\hbar$ explaining perhaps in part the strong hindrance (10^4 to 10^7) deduced for the observed transition if one bases oneself on Goldanskii's estimate of about 1 µsec for Q_p = 1.2 and Z = 71.

5. Outlook

In the course of this work a large number of new isotopes could be unambiguously identified. One of the results was a substantial broadening of the Q_α systematics in the region N = 84 to 92. An important progress in the study of α decay is the development of a reliable parent-daughter correlation method allowing to determine relatively accurate α branching ratios of very short lived nuclear species having small production cross sections. Much needs to be done yet: in order to obtain useful information for the more detailed interpretation of reduced α-widths and the structural effects that govern their variation over large Z and A ranges, still more accurate measurements of half lives and branching ratios are necessary: this will require the shift from the more survey type of experiments presented here to experiments devoted more specifically to given isotopes with more accelerator time spent at a given point.

The discovery of proton radioactivity opens up a new prospect of getting rather specific nuclear structure information for nuclei very far from the ß-stability line, where production cross sections tend to be rather low and where detailed γ spectroscopy would be exceedingly difficult. The theory of proton decay, despite the complications of spin orbit coupling, should be in many ways more transparent, especially in terms of absolute decay probabilities, than the

α decay theory due to the single nucleon nature of the proton.

The authors acknowledge with pleasure the help of many groups which supported our experiments. Especially we thank the accelerator group for providing excellent beams and the target laboratory for producing our targets. Data collection and data analysis have become possible by the achievements of the program development group of the GSI computer center.

References

1. Hansen, P.G.: Ann.Rev. of Nucl. and Particle Science, 29, 69 (1979)

2. LeBeyec, Y.: Inst. de Phys. Nucl., Orsay, Report, R.C. 79-1o

3. Ravn, H.L.: Proc. 3rd Int. Conf. on Nuclei far from Stability, Cargèse, CERN 76-13,22(1976)

4. Münzenberg, G., Faust, W., Hofmann, S., Armbruster, P., Güttner, K., Ewald, H.: Nucl. Inst. Meth. 161,65(1979)

5. Faust, W.: Das Geschwindigkeitsfilter SHIP - Beschreibung, Ausmessung, Berechnung des Wirkungsgrades und erste Experimente, Thesis, GSI-P-4-78(1978)

6. Northcliffe, L.C., Schilling, R.F.: Nuclear Data Tables A7,233(197o)

7. Hofmann, S., Faust, W., Münzenberg, G., Reisdorf, W., Armbruster, P., Güttner, K., Ewald, H: Z. Physik A291,53(1979)

8. Hofmann, S., Münzenberg, G., Heßberger, F., Reisdorf, W., Armbruster, P., Thuma, B.: Z. Phys. A299,281(1981)

9. Wapstra, A.H., Bos, K.: Atomic Data and Nuclear Data Tables 19, No.3(1977).

1o. Harmatz, B.: Nuclear Data Sheets 19,33(1976)

11. Bowman, J.D., Hyde, E.K., Eppley, R.E.: Lawrence Berkeley Laboratory, Nuclear Chemistry Annual Report No. LBL-1666 p.4(1972)

12. Toth, K.S., Hahn, R.L., Bingham, C.R., Ijaz, M.A., Walker, R.F.: Phys.Rev. C7,2o1o(1973)

13. Eastham, D.A., Grant, I.S.: Nucl. Phys. A2o8, 119(1973)

14. Toth, K.S., Schmidt-Ott, W.-D., Bingham, C.R., Ijaz, M.A.: Phys. Rev. C12,533(1975)

15. Hagberg, E., Hansen, P.G., Hardy, J.C., Hornshøj, P., Jonson, B., Mattsson, S., Tidemand-Petersson, P.: Nucl. Phys. A293,1

16. Cabot, C., Della Negra, S., Deprin, C., Gauvin, H., LeBeyec, Y.: Z. Physik A287,71(1978)

17. Gauvin, H., LeBeyec, Y., Livet, J., Reyss, J.L.: Ann. Phys. 9,241(1975)

18. Takahashi, K., Yamada, M., Kondoh, T.: Atomic Data and Nucl. Data Tables 12,1o1(1973)

19. Maripuu, S. (ed.): 1975 Mass Predictions, Atomic Data and Nuclear Data Tables 17, Nos. 5-6, 476(1976)

2o. Möller, P., Nix, J.R.: Nuclear Mass Formula with Yukawa -Plus- Exponential Macroscopic Model and α Folded-Yukawa Single-Particle Potential, Preprint LA-UR-8o-1996(198o)

21. Rasmussen, J.O.: Phys. Rev. 113,1593(1959)

22. Burrows, T.W.: Nucl. Data Sheets 12,2o3(1974)

23. Burrows, T.W.: Nucl. Data Sheets 14,413(1975)

24. Burrows, T.W., Auble, R.L.: Nucl. Data Sheets 16,231(1975)

25. Baglin, C.M.: Nucl. Data Sheets 18,223(1976)

26. Harmatz, B.: Nucl. Data Sheets 19,33(1976)

27. Holland, G.E.: Nucl, Data Sheets 19,337(1976)

28. Harmatz, B., Shepard, J.R.: Nucl. Data Sheets 2o,373 (1977)

29. Harmatz, B., Ewbank, W.B.: Nucl. Data Sheets 25, 113(1978)

3o. Macfarlane, R.D., Rasmussen, J.O., Rho, M.: Phys. Rev. 134, 1196(1964)

31. Mang, H.J.: Ann. Rev. Nucl. Science 14,1(1964)

32. Broda, R., Ogawa, M., Lunardi, S., Maier, M.R., Daly, P.J., Kleinheinz, P.: Z. Physik A285,423(1978)

33. Daly, P.J., Kleinheinz, P., Broda, R., Stefanini, A.M., Lunardi, S., Backe, H., Richter, L., Willwater, R., Weik, F.: Z. Phys. A288, 1o3(1978)

34. Kleinheinz, P., Ogawa, M., Broda, R., Daly, P.J., Haenni, D., Beuscher, H., Kleinrahm, A.: Z. Physik A286,27(1978

35. Goldanskii, V.I.: Ann. Rev. Nucl. Sci,16,1(1966)

36. Jackson, K.P., Cardinal, C.U., Evans, H.C., Jelley, N.A., Cerny, J.: Phys. Lett. 33B,281(197o)

37. Hardy, J.C.: Ann. Rev. of Nucl. and Part. Science 29,417(1979)

38. Myers, W.D.: Droplet Model of Atomic Nuclei, Plenum, New York(1977)

DISCUSSION

G. Rudstam: What is the statistical accuracy of the 1.19 MeV line in the excitation function used to assign it to a specific nuclide?

S. Hofmann: Statistical errors of the points are smaller than the point size. Systematic errors due to efficiency calibration may shift the excitation functions in the vertical direction but as a whole so that the form of the curves will be conserved.